Journal of Engineering Physics and Thermophysics, Vol. 77, No. 3, 2004

MATHEMATICAL MODELING OF THE HEAT EXCHANGE OF THE PAYLOAD MODULE OF NONHERMETIC GEOSTATIONARY SPACECRAFT

V. A. Burakov,[a] **V. V. Elizarov,**[a]
V. P. Kozhukhov,[b] **E. N. Korchagin,**[b]
A. S. Tkachenko,[a] **and I. V. Shcherbakova**[a]

UDC 629.78.048.7.001.24

Dynamic thermal mathematical models in lumped and distributed-lumped parameters, computational algorithms, software, and results of comparative numerical calculations of the processes of radiative-conductive heat exchange of the payload module of prospective nonhermetic block-modular geostationary spacecraft with a long service life under the conditions of orbital operation have been presented.

A new generation of competitive nonhermetic geostationary spacecraft (NS) with a long service life (no shorter than 12 years) is under development at present. In such spacecraft, use is made of a large-scale "box"-shaped nonhermetic instrument compartment representing a block-modular structure of plane rectangular three-layer honeycomb panels, carrying thermally loaded onboard equipment (OE), and performing force, thermal, and protective (against ionizing radiations) functions simultaneously [1]. One structural layout of the nonhermetic instrument compartment, which is nontraditional for Russian spacecraft, consists of the payload module and the service-systems module [2]. The payload module (PM) (Fig. 1) consists of a П-block including the North and South (instrument-radiator) panels, the Central panel, the East and West removable covers, and the engine-block panel (EBP) shared with the service-systems module. A passive thermal-regulation system based on optical coatings in combination with systems of electric heating and unregulated low-temperature heat pipes (HPs) of different configurations and profile types, which thermally connect the North and South radiator panels, is used to ensure the thermal regime of the onboard equipment.

Taking into account the insufficient experience gained in designing and the limited possibilities of full-scale experimental trial in thermal-vacuum tests, one imposed stringent requirements on the accuracy of the design parameters of the thermal regimes of the onboard devices, the thermal state of structural elements, and the sufficiency of the passive thermal-regulation system under actual conditions of orbital operation of geostationary NS.

In accordance with the classification of [3], one can make such thermal analyses by the dynamic thermal mathematical models in lumped parameters (lumped-parameter thermal mathematical models (LPTMMs)), in distributed-lumped parameters (distributed-lumped-parameter thermal mathematical models (DLPTMMs)), and in distributed parameters (distributed-parameter thermal mathematical models (DPTMMs)). The LPTMMs referring to the first-level models are nonlinear systems of ordinary differential heat-balance equations. The DLPTMMs represent second-level models in which use is made of both heat-balance equations and one-, two-, and three-dimensional nonstationary heat-transfer equations in partial derivatives. The DPTMMs are third-level models reflecting most completely the physical essence of heat-exchange processes with the use of just partial equations. One uses the LPTMMs universally to obtain calculated design parameters; the DLPTMMs are used less frequently, whereas the DPTMMs are used only in exceptional cases.

The LPTMMs enable one to carry out multiparametric prediction and optimization at different stages of designing with a minimum consumption of computer time. The main difficulty associated with the employment of the LPTMMs lies in selection of the minimum number of subdivisions (computational nodes) and computations of the right-hand sides of the system of heat-balance equations, ensuring the desired accuracy of calculation of the tempera-

[a]Scientific-Research Institute of Applied Mathematics and Mechanics at Tomsk State University, Tomsk, Russia; [b]M. F. Reshetov Scientific-Production Association of Applied Mechanics, Zheleznogorsk, Russia. Translated from Inzhenerno-Fizicheskii Zhurnal, Vol. 77, No. 3, pp. 108–116, May–June, 2004. Original article submitted November 26, 2002.

1062-0125/04/7703-0595

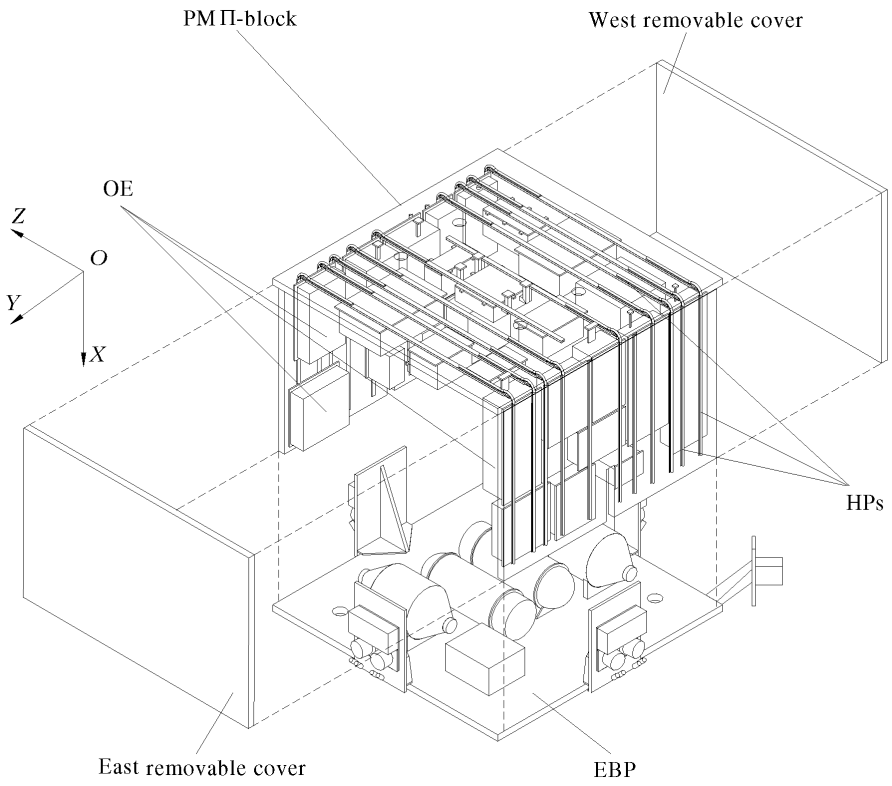

Fig. 1. General block-modular scheme of the payload module of the nonhermetic instrument compartment of a spacecraft with a long service life. *OXYZ*, global coordinate system.

ture-field distribution. The minimum number of subdivisions depends on the degree of nonuniformity of the temperature fields and, generally speaking, cannot be selected a priori. In this connection, the calculations by the LPTMMs always need to be checked by comparing them to those by more complex mathematical models or to experimental data.

This work seeks to mathematically model the radiative-conductive heat exchange of the payload module of geostationary NS under the conditions of orbital operation with the use of traditional LPTMMs and more complex DLPTMMs.

The most important mechanisms of radiative-conductive heat exchange of the payload module of geostationary NS under the conditions of orbital operation are:

(a) external radiative heat exchange on the North and South instrument-radiator panels and East and West removable covers;

(b) internal radiative heat exchange;

(c) heat transfer in the heat-releasing onboard devices;

(d) conductive heat transfer in the three-layer honeycomb panels;

(e) heat and mass transfer in the passive thermal-regulation system based in heat pipes;

(f) contact heat exchange.

The external and internal radiative heat exchange of the payload module of a geostationary NS in orbital operation is calculated according to the procedures proposed earlier [2].

Different mathematical models in distributed and lumped parameters have been developed for analysis of the heat transfer and thermal regimes of the onboard devices [4]. For routine extremum evaluations it is assumed in the present work that the total heat released in operation of the onboard equipment is supplied to the mounting surface (hypothesis for the mounting site of a device [2]).

The dynamic LPTMMs of conductive heat transfer in the instrument-radiator and other types of three-layer honeycomb panels of the payload modules of geostationary NS with allowance for the special properties of their external and internal heat exchange in orbital operation have the form

$$P_i(t) + E_{ri}F_i = C_{1i}\frac{dT_{1i}}{dt} + \sigma_{1im}(T_{1i} - T_{1m}) + \sigma_{12}(T_{1i} - T_{2i}) + \sigma_{\text{f.st}1i}(T_{1i} - T_{\text{st}i}) + \\ + \sigma_{\text{f.p}i}(T_{1i} - T_{\text{v}}), \quad i = \overline{1, N_xN_y}; \tag{1}$$

$$q_{\text{s}}(t)F_i + \sigma_{12}(T_{1i} - T_{2i}) + \sigma_{\text{f.st}i}(T_{\text{st}i} - T_{2i}) = C_{2i}\frac{dT_{2i}}{dt} + \sigma_{2im}(T_{2i} - T_{2m}) + \varepsilon_2\sigma_0T_{2i}^4F_i, \quad i = \overline{1, N_xN_y}; \tag{2}$$

$$\sigma_{\text{f.st}i}(T_{1i} - T_{\text{st}i}) = C_{\text{st}i}\frac{dT_{\text{st}i}}{dt} + \sigma_{\text{st}2i}(T_{\text{st}i} - T_{2i}) + \sigma_{\text{st,cont}}(T_{\text{st}i} - T_{\text{st}i\text{cont}}), \\ i = \overline{1, 2(N_xN_y)}; \tag{3}$$

$$T_{1i}(0) = T_{2i}(0) = T_{\text{st}i}(0) = T_{\text{int}}, \tag{4}$$

and represent the systems of $2(N_xN_y + N_x + N_y)$ ordinary differential heat-balance equations (1)–(3) with corresponding boundary conditions (4).

Mathematical modeling of heat transfer in single-shelf unregulated heat pipes built into an anisotropic honeycomb filler on the interior facings (linings) of the North, Central, and South panels is carried out within the framework of the conductive (disregarding the detailed analysis of the hydrodynamics and heat and mass transfer in a vapor channel) dynamic LPTMMs under the following main assumptions:

(1) a single heat pipe or a bundle of two or three heat pipes operates in the subcritical regime (absence of hydrodynamic choking, boiling, and freezing of the heat-transfer agent);

(2) transfer of heat in the heat-pipe structural elements in the axial and circular directions is insignificant;

(3) the vapor is in the saturation state and its temperature along the heat pipe is constant;

(4) the zones of evaporation and condensation of the heat pipe coincide with the longitudinal dimensions of the mounting sites of the onboard devices and the lengths of joint of two heat pipes into a bundle;

(5) the coefficient of heat transfer in phase transformations of the heat-transfer agent in the evaporation and condensation zones of the heat pipe are constant.

The dynamic conductive LPTMM of a bundle of three heat pipes, which thermally connects the South and North instrument-radiator panels of the payload Π-module represents a system of ordinary differential heat-balance equations with corresponding boundary conditions:

$$\sigma_{\text{f.p}1n}(T_{11n} - T_{\text{e}1n}) = C_{\text{e}1n}\frac{dT_{\text{e}1n}}{dt} + \sigma_{\text{e}11n}(T_{\text{e}1n} - T_{\text{v}1}), \\ \sigma_{\text{c}1}(T_{\text{v}1} - T_{\text{c}1}) = C_{\text{c}1}\frac{dT_{\text{c}1}}{dt} + \sigma_{\text{p.p}12}(T_{\text{c}1} - T_{\text{e}2}), \\ T_{\text{e}1n}(0) = T_{\text{c}1}(0) = T_{\text{int}}, \\ \sigma_{\text{p.p}12}(T_{\text{c}1} - T_{\text{e}2}) = C_{\text{e}2}\frac{dT_{\text{e}2}}{dt} + \sigma_{\text{e}2}(T_{\text{e}2} - T_{\text{v}2}), \tag{5}$$

$$\sigma_{\text{f.p2}n}\,(T_{12n}-T_{\text{e2}n})=C_{\text{e2}n}\,\frac{dT_{\text{e2}n}}{dt}+\sigma_{\text{e22}n}\,(T_{\text{e2}n}-T_{\text{v2}})\,,$$

$$\sigma_{\text{c2}}\,(T_{\text{v2}}-T_{\text{c2}})=C_{\text{c2}}\,\frac{dT_{\text{c2}}}{dt}+\sigma_{\text{p.p23}}\,(T_{\text{c2}}-T_{\text{e3}})\,, \tag{6}$$

$$T_{\text{e2}}\,(0)=T_{\text{e2}n}\,(0)=T_{\text{c2}}\,(0)=T_{\text{int}}\,,$$

$$\sigma_{\text{p.p23}}\,(T_{\text{c2}}-T_{\text{e3}})=C_{\text{e3}n}\,\frac{dT_{\text{e3}n}}{dt}+\sigma_{\text{f.p3}n}\,(T_{\text{c3}n}-T_{13n})\,,$$

$$\sigma_{\text{c33}n}\,(T_{\text{v3}}-T_{\text{c3}n})=C_{\text{c3}n}\,\frac{dT_{\text{c3}n}}{dt}+\sigma_{\text{f.p3}n}\,(T_{\text{c3}n}-T_{13n})\,, \tag{7}$$

$$T_{\text{e3}}\,(0)=T_{\text{c3}n}\,(0)=T_{\text{int}}\,.$$

The system of equations (5)–(7) is open, since we do not know the temperature of the saturated vapor in the bundle of three heat pipes. The closure condition is formulated based on the law of conservation of energy in the vapor channel of the heat pipe in the known quasistationary form

$$\sum_{n}\,\sigma_{\text{e1}n}\,(T_{\text{e1}n}-T_{\text{v1}})+\sigma_{\text{c1}}\,(T_{\text{c1}}-T_{\text{v1}})=0\,, \tag{8}$$

$$\sigma_{\text{e2}}\,(T_{\text{e2}}-T_{\text{v2}})+\sum_{n}\,\sigma_{\text{e22}n}\,(T_{\text{e2}n}-T_{\text{v2}})+\sigma_{\text{c2}}\,(T_{\text{c2}}-T_{\text{v2}})=0\,, \tag{9}$$

$$\sigma_{\text{e3}}\,(T_{\text{e3}}-T_{\text{v3}})=\sum_{n}\,\sigma_{\text{c33}n}\,(T_{\text{c33}n}-T_{\text{v3}})=0\,. \tag{10}$$

The system of equations (5)–(7) and closing relations (8)–(10) is extended to a bundle of two heat pipes and a single heat pipe that are also part of the heat-pipe network in the panels of the payload Π-module.

Contact heat exchange is important in detachable and permanent joints of homogeneous and heterogeneous structural elements of a nonhermetic instrument compartment. Methods of calculation of the coefficients of contact thermal conductivity (they are the reciprocals of specific thermal resistance) for certain kinds of joints are known [5, 6]. However, it is noteworthy that these coefficients are distinguished by a considerable uncertainty before full-scale thermal-vacuum tests.

Time-varying temperature fields at the computational nodes of all the panels and the passive thermal-regulation system based on the network of unregulated heat pipes are a result of the mathematical modeling of radiative-conductive heat exchange of the payload module of geostationary NS under conditions of orbital operation within the framework of the dynamic LPTMM (1)–(10).

Within the framework of the assumptions made [2], the dynamic DPTMMs of conductive heat transfer in the instrument-radiator and other types of three-layer honeycomb panels of the payload module with allowance for the special properties of their external and internal heat exchange in orbital operation have the form (in a Cartesian coordinate system)

$$\frac{\partial T_m}{\partial t}=a_{\text{f}}\left(\frac{\partial^2 T_m}{\partial x^2}+\frac{\partial^2 T_m}{\partial y^2}\right)+Q_m\,,\quad m=1,\,2\,,\quad 0<x<L_x\,,\quad 0<y<L_y\,,\quad 0<t\le 24\text{ h}\,; \tag{11}$$

$$\frac{\partial T_m}{\partial t} = a_{\text{st}} \frac{\partial^2 T_m}{\partial \xi^2} + \Phi_m + \Phi_{m\text{cont}}, \quad m = \overline{3, 6}, \quad 0 < \xi < 2\,(L_x + L_y), \quad 0 < t \le 24 \text{ h}; \tag{12}$$

$$\left.\frac{\partial T_m}{\partial n}\right|_{\Gamma_m} = 0, \quad m = 1, 2; \tag{13}$$

$$\left.\frac{\partial T_3}{\partial \xi}\right|_{\xi=L_y} = \left.\frac{\partial T_4}{\partial \xi}\right|_{\xi=L_y}, \quad T_3\big|_{\xi=L_y} = T_4\big|_{\xi=L_y}, \tag{14}$$

$$\left.\frac{\partial T_4}{\partial \xi}\right|_{\xi=L_y+L_x} = \left.\frac{\partial T_5}{\partial \xi}\right|_{\xi=L_y+L_x}, \quad T_4\big|_{\xi=L_y} = T_5\big|_{\xi=L_y+L_x}, \tag{15}$$

$$\left.\frac{\partial T_5}{\partial \xi}\right|_{\xi=2L_y+L_x} = \left.\frac{\partial T_6}{\partial \xi}\right|_{\xi=2L_y+L_x}, \quad T_5\big|_{\xi=L_y} = T_6\big|_{\xi=2L_y+L_x}, \tag{16}$$

$$\left.\frac{\partial T_3}{\partial \xi}\right|_{\xi=0} = \left.\frac{\partial T_6}{\partial \xi}\right|_{\xi=2(L_y+L_x)}, \quad T_3\big|_{\xi=0} = T_6\big|_{\xi=2(L_x+L_y)}; \tag{17}$$

$$T_m(x, y, 0) = T_{\text{int}}, \quad m = 1, 2, \quad 0 \le x \le L_x, \quad 0 \le y \le L_y; \tag{18}$$

$$T_m(\xi, 0) = T_{\text{int}}, \quad m = \overline{3, 6}, \quad 0 \le \xi \le 2\,(L_x + L_y). \tag{19}$$

The dynamic DPTMM (11)–(19) describes conductive heat transfer in six basic elements of the three-layer honeycomb panel: the load-bearing metallic facings (11) and the skeleton elements (12) with boundary and initial conditions (13)–(19). The origin of coordinates $\xi = 0$ coincides with the origin of the Cartesian coordinate system. The skeleton elements are numbered in the direction of the *OY* axis. Boundary condition (19) corresponds to the periodic problem of nonstationary heat conduction.

The dynamic LPTMM of three-layer honeycomb panels (11)–(19) is closed by determination of the source terms Q_{m}, Φ_m, and $\Phi_{m\text{cont}}$ in the equations of nonstationary heat conduction (11) and (12), which are responsible for external, internal, and contact heat exchange:

$$Q_1 = \frac{\sum\limits_n q_{\text{s}.en} + E_{\text{r}1} - q_{\text{cond}1} - \sum\limits_k q_{\text{h}.pk} - q_{\text{f.st}1}}{\delta_{\text{f}1}\,\rho_{\text{f}} c_{\text{f}}}, \tag{20}$$

$$q_{\text{s}.en}(x, y, t) = \frac{P_{\text{s}.en}(x, y, t)}{F_{\text{s}.en}}, \quad n = \overline{1, N_{\text{s.e}}},$$

$$q_{\text{h}.pk}(x, y, t) = \alpha_{\text{f}.pk}\,[T_1(x, y, t) - T_{vk}(t)], \quad k = \overline{1, N_{\text{h.p}}},$$

$$q_{\text{f.st}1} = \alpha_{\text{f.st}}\,[T_1(0, y, t) + T_1(x, L_y, t) + T_1(L_x, y, t) + T_1(x, 0, t) - (T_3 + T_4 + T_5 + T_6)];$$

$$Q_2 = \frac{q_s(t) + q_{cond2} - \varepsilon_2 \sigma_0 T_2^4 - q_{f.st2}}{\delta_{f2}\,\rho_f c_f}, \tag{21}$$

$$q_{cond1} = q_{cond2} = \frac{\lambda_{eff}}{\delta_h}\left(\frac{Bi_{f.h}}{1 + Bi_{f.h}}\right)(T_1 - T_2),$$

$$q_{f.st2} = \alpha_{f.st}\,[T_2(0, y, t) + T_2(x, L_y, t) + T_2(L_x, y, t) + T_2(x, 0, t) - (T_3 + T_4 + T_5 + T_6)];$$

$$\Phi_3 = \frac{\alpha_{f.st}\,[T_1(0, y, t) + T_2(0, y, t) - 2T_3]}{h_{st}\,\rho_{st} c_{st}}, \tag{22}$$

$$\Phi_{3c} = -\frac{\alpha_{cont}\,(\bar{T}_3 - \bar{T}_{3cont})}{\delta_{st}\,\rho_{st} c_{st}}; \tag{23}$$

.....

$$\Phi_6 = \frac{\alpha_{f.st}\,[T_1(x, 0, t) + T_2(x, 0, t) - 2T_6]}{h_{st}\,\rho_{st} c_{st}}, \tag{24}$$

$$\Phi_{6c} = -\frac{\alpha_{cont}\,(\bar{T}_6 - \bar{T}_{6cont})}{\delta_{st}\,\rho_{st} c_{st}}, \tag{25}$$

where $\bar{T}_{m\text{cont}}$ is the mean-integral temperature of the zone of metallic facing of the opposite panel which is in contact with the mth element of the skeleton.

Coordinate- and time-dependent multidimensional nonstationary fields of temperatures of all the three-layer honeycomb panels of the structure and time-varying temperatures at the computational models of the passive thermal-regulation system based on unregulated heat pipes are a result of the mathematical modeling of the radiative-conductive heat transfer of the module of geostationary NS under the conditions of orbital operation within the framework of the dynamic DLPTMM (11)–(25), (5)–(10).

Computer modeling (by an LPTMM) of the payload module of an NS has been carried out with use of a two-step predictor–corrector scheme of second order of accuracy in time, which requires no iterations [7]. Numerical realization of the nonstationary equations of heat conduction in the load-bearing metallic facings (11) has been carried out by the finite-difference method according to an economic noniterative two-layer scheme of component-by-component splitting (fractional steps) with N. N. Yanenko's balance [7] on a fixed irregular grid; in the skeleton elements (12), it has been carried out along the marching coordinate by the cyclic-running method [8]. We have created a procedure of automatic generation of the irregular grid (the procedure includes construction of a geometric grid separating, in accordance with the drawing, all the inhomogeneities (mounting sites of devices, lines of laying of heat pipes, and zones covered with shield-vacuum heat insulation) inherent in a given thermal problem) and a finer grid for calculation of nonstationary conductive heat transfer and construction of a system of isothermal area elements for calculation of internal radiative heat exchange by the zonal method [2]. Versions of the MPN-S and MPN 1 computer programs have been developed for IBM-compatible personal computers in the high-level algorithmic language Visual C^{++} (v. 6.0). The computations were monitored on each time layer by checking the total integral balance of heat in the three-layer honeycomb panels and the entire payload module as an assembly with allowance for contact heat exchange, the local heat balances at the mounting sites of the onboard devices, the integral heat balance in the passive thermal-regulation system based on a network of unregulated heat pipes, and the law of conservation of radiant energy in calculation of the internal radiative heat exchange. In a diurnal cycle of illumination by the sun, the typical time of calculation of one vari-

39.5	40.1	39.9	32.1	31.4
21.5	21.8	15.3	18.3	18.6
23.5	23.9	20.3	17.2	15.7
14.6	14.8	14.4	11.9	7.8
9.5	9.6	9.6	9.4	6.3

29.5	32.3	31.0	32.8	22.9
20.0	20.5	20.1	21.7	17.2
21.1	19.8	18.7	25.1	11.8
17.6	19.7	15.4	9.5	5.4
10.8	11.6	9.4	7.4	3.2

5.5	6.1	0.1	4.7	4.6	
3.7	3.9	-9.0	-2.0	-2.9	
12.1	13.0	5.0	3.4	-9.8	*I*
18.9	19.9	11.1	7.07	6.1	
27.5	28.7	18.8	22.1	21.8	

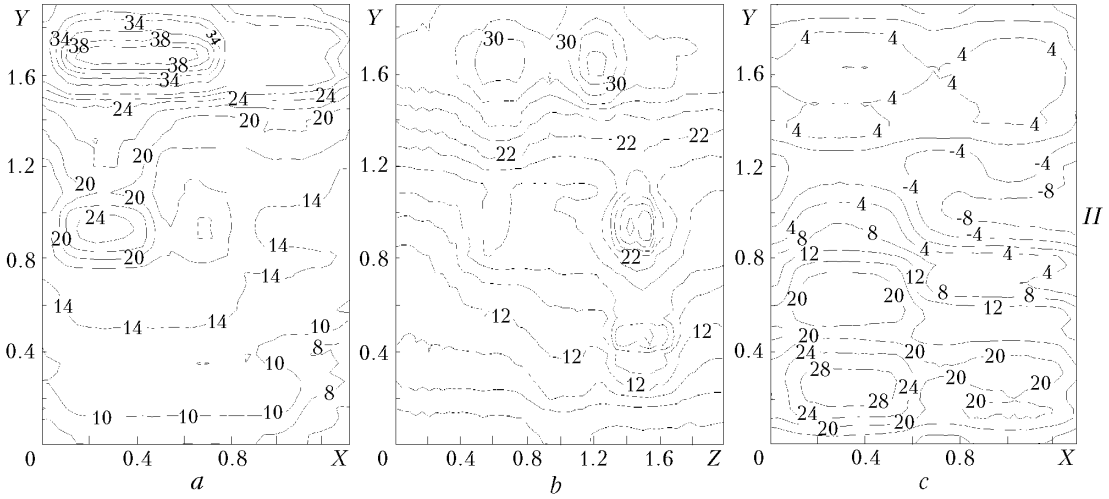

Fig. 2. Temperature distribution of the metallic facings of the instrument sides of the South (a), Central (b), and North (c) panels: *I*, LPTMM; *II*, DLPTMM. *T*, °C; *X*, *Y*, *Z*, m.

ant on a Pentium III personal computer (733 MHz) according to the MPN-S program was 3.5 min for a number of nodes of 420 (payload module) and 211 (passive thermal-regulation system) with time steps of τ = 20 sec (payload module) and τ = 0.5 sec (passive thermal-regulation system), which is quite acceptable for multiparametric and optimization calculations. The accuracy for the integral heat balance in the three-layer honeycomb panels was very high: 0.02 W in the passive thermal-regulation system based on a network of unregulated heat pipes and 0.3 W in the payload module as an assembly; in the calculation of the internal radiative heat exchange, it was no worse than 0.3–0.7 W.

Under the same conditions, the typical time of calculation of one variant on a Pentium III personal computer (733 MHz) according to the MPN-1 program was about 8 min for 33 × 71 (South panel), 43 × 67 (Central panel), 31 × 74 (North panel), and 25 × 50 (East and West radiator panels and the engine-block panel) finite-difference grids and with time steps of τ = 20 sec (payload module) and τ = 0.05 sec (passive thermal-regulation system). The accuracy for the integral heat balance on the panels and the local heat balance at the mounting sites of the devices was no worse than 2.5 and 6% respectively. The law of conservation of radiant energy was valid with an accuracy of no less than 0.35 W.

The results of the numerical calculations of the radiative-conductive heat exchange of geostationary NS according to the MPN-S and MPN-1 computer programs were processed with the use of modern technologies of graphic and multiplication visualization and of high-quality color computer animation.

According to the MPN-S (LPTMM) and MPN-1 (DLPTMM) programs and with the use of a Pentium III personal computer, we calculated numerically the radiative-conductive heat exchange of a prospective geostationary NS with a long service life and a total heat release of the onboard equipment of 1072 W. A network of unregulated am-

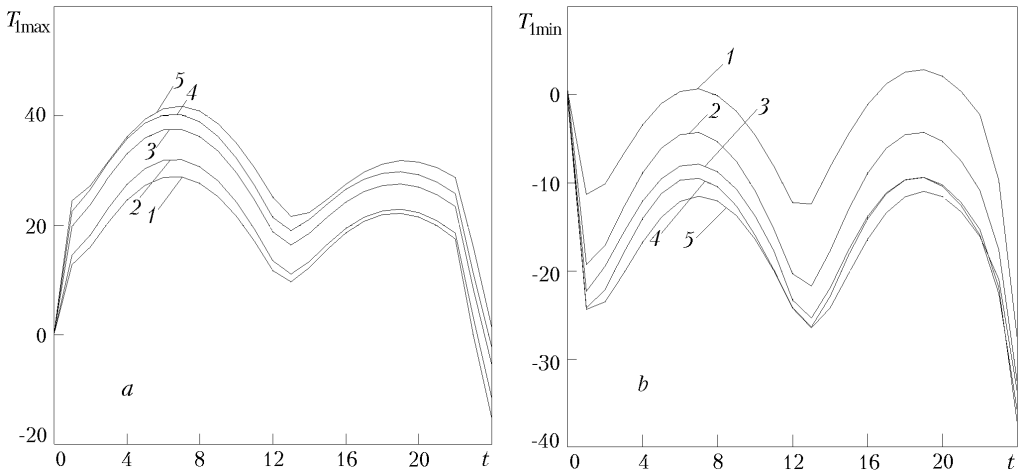

Fig. 3. Dynamics of change of the maximum and minimum temperatures of metallic facings of the mounting sites of the onboard devices of the South (a) and North (b) radiator panels: 1) 2 × 2; 2) 3 × 3; 3) 4 × 4; 4) 5 × 5; 5) DLPTMM. T_{1max} and T_{1min}, ^{o}C; t, h.

monia heat pipes of a single-shelf profile (AS-CRA 7.5-R1), manufactured from AD-31-T5 aluminum alloy according to the All-Union State Standard 4784-74, with a cylindrical grooved capillary structure developed at the Laboratory of Heat Pipes of the National Technical University of Ukraine "Kiev Polytechnic Institute" was used as the passive thermal-regulation system. Extremum conditions of orbital operation at the end of a 15-year period of active life (A_s = 0.4 and θ = 66.5^{o}) at the point of vernal equinox (S_0 = 1400 W/m^2) in the diurnal cycle of illumination by the sun $0 < t \le 22.8$ h and the shadow portion of the earth $22.8 < t < 24$ h were considered. The time was calculated from the beginning of the illumination of the East removable cover. We employed the following set of initial data:

linear dimensions of:

(a) the South and North radiator panels of the payload module 1.3 × 1.9 × 0.5 m;

(b) the Central (facing the earth) panel of the payload module 2 × 2 × 0.05 m;

(c) the East and West removable covers of the payload module 1.3 × 2 × 0.05 m;

(d) the engine-block panel 2 × 2 × 0.05 m;

$\delta_{f1} = \delta_{f2} = 10^{-3}$ m;

ρ_f = 2700 kg/m^3; c_f = 880 J/(kg·K); λ_f = 130 W/(m·K);

$\delta_h = 48 \cdot 10^{-3}$ m;

λ_{eff} = 1.48 W/(m·K) (foil thickness $4 \cdot 10^{-5}$ m; size of the honeycomb cell $5 \cdot 10^{-3}$; thermal conductivity of the material 120 W/(m·K));

parameters of the heat pipes in the payload module: outside diameter $14 \cdot 10^{-3}$ m, inside diameter $12 \cdot 10^{-3}$ m, width of the shelf 0.03 m, running mass 0.31 kg/m, and coefficients of heat transfer in phase transformations in the evaporation and condensation zones 7000 W/(m^2·K);

specific thermal resistance of:

(a) the adhesive joint of the heat-pipe shelf and the panel facing $4 \cdot 10^{-3}$ (m^2·K)/W;

(b) the adhesive joint of the heat pipes via the shelves 10^{-3} (m^2·K)/W; joint length 0.3 m;

(c) the adhesive joint between the facing and the honeycomb filler 10^{-3} (m^2·K)/W;

(d) the facing and the skeleton elements 0.14 (m^2·K)/W;

(e) the junctions of the honeycomb panels of the instrument-compartment structure 0.02 (m^2·K)/W;

coefficient of absorption of direct solar radiation of the removable covers of the payload module 0.425;

integral emissive power of:

(a) the radiative surfaces of the South and North radiator panels of the payload module 0.85;

(b) the radiative surfaces of the East and West removable covers of the payload module 0.85;

(c) the interior surfaces of the payload module 0.82;

initial temperature 0^{o}C.

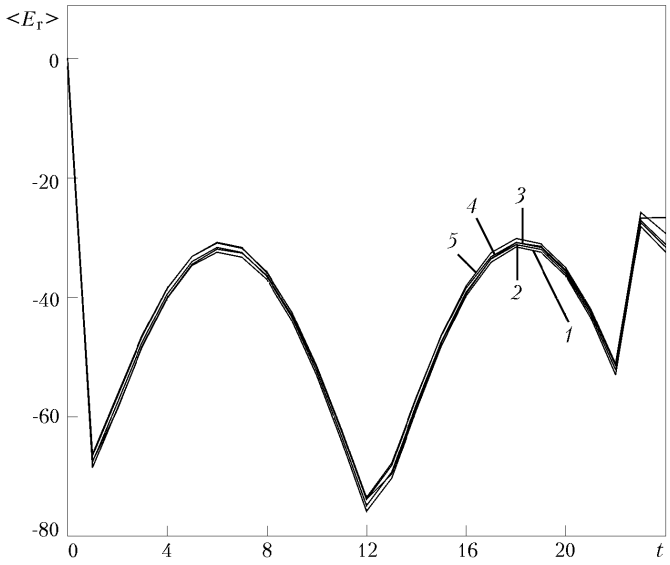

Fig. 4. Dynamics of change of the average resulting internal radiative heat fluxes on the South radiator panel: 1) 2 × 2; 2) 3 × 3; 3) 4 × 4; 4) 5 × 5; 5) DLPTMM. E_r, W/m^2; t, h.

Figure 2 shows the general character of change of the temperature fields of the metallic facings of the South, Central, and North panels in subdivision into 5 × 5 computational nodes (LPTMM) and corresponding isotherms (DLPTMM) at the instant of time t = 6 h. As is seen, despite the presence of thermal inhomogeneities (the mounting sites of the onboard devices and the network of operating heat pipes), we have a fairly good qualitative and quantitative agreement of the results of numerical calculations of the conductive heat transfer in the panels with onboard devices, obtained according to the dynamic LPTMMs and DLPTMMs. For the South and North radiator panels and the Central panel the disagreement between the LPTMM and DLPTMM for the local maximum and minimum temperatures at the mounting sites of the onboard devices in the case of subdivision into 5 × 5 computational grids and for t = 6 h was −1.2, −1.5, and −2.0°C and −0.5, 1.6, and 2.8°C. A typical character of the influence of the number of subdivisions on the dynamics of change of the local maximum and minimum temperatures of the metallic facing at the mounting sites of the onboard devices of the South and North radiator panels in the diurnal cycle of illumination by the sun with allowance for the shadow portion of the earth is presented in Fig. 3. Further increase in the number of subdivisions to 10 × 10 had virtually no effect on the improvement in the accuracy of calculations according to the LPTMM, i.e., a number of subdivisions of 5 × 5 can be taken as the minimum optimum number of computational nodes for this structure of the payload module. On the North radiator panel, the range of minimum temperatures on the shadow portion of the earth goes beyond the permissible range of temperatures of normal operation of the onboard devices (−20°C) and additional electric heating is required. As was to be expected, the influence of the number of subdivisions on the dynamics of the average temperatures of the metallic facings of the instrument sides of the South and North radiator panels and the Central panel of the payload module turned out to be less appreciable and the disagreement of the results obtained according to the LPTMM (5 × 5) and DLPTMM was 0.8, 0.3, and 0.6°C for t = 6 h.

The dynamics of change of the average resulting internal radiative fluxes on the instrument metallic facings of the South radiator panel in the diurnal cycle of illumination by the sun and the shadow portion of the earth versus the number of subdivisions is shown in Fig. 4. The maximum difference between the LPTMM (5 × 5) and the DLPTMM for t = 6 h was equal to −0.5 W/m^2 and was 0.7 and −1.5 W/m^2 respectively for the North radiator panel and the Central panel.

The results of numerical calculations of the saturated-vapor temperatures in the passive thermal-regulation system based on a network of single-shelf unregulated ammonia heat pipes, which have been obtained according to the dynamic LPTMM (5 × 5) and DLPTMM at the instant of time t = 6 h, are summarized in Table 1. Here the maximum disagreements for the network of heat pipes laid in the South and North radiator panels and the Central panel were −3.8, −4.0, and 4.6°C.

TABLE 1. Temperatures of the Saturated Vapor of Heat Pipes T_v, ^oC, in the Payload Π-Module, Obtained According to the LPTMM and DLPTMM

Panel	Heat-pipe No.	Model	
		LPTMM	DLPTMM
South	11	34.3	32.0
	10	34.1	31.0
	9	18.2	22.0
	8	20.1	21.3
	7	17.7	16.9
	6	21.0	18.8
	5	13.4	14.3
	4	13.9	13.1
	3	8.1	10.4
	2	8.8	11.2
	1	8.5	8.2
Central	10	31.4	29.8
	9	31.3	29.3
	8	18.2	22.0
	7	20.0	21.9
	6	16.2	16.8
	5	20.9	19.2
	4	13.6	12.6
	3	8.1	10.5
	2	8.4	10.8
	1	7.7	6.5
North	1	28.0	26.1
	2	27.9	26.9
	3	15.7	19.6
	4	19.4	21.7
	5	12.9	14.4
	6	1.1	–3.6
	7	0.9	–1.8
	8	10.4	9.9
	9	6.5	7.8
	10	6.6	8.7
	11	6.2	4.3

Thus, mathematical modeling of the radiative-conductive heat transfer of the payload module of prospective NS with a long service life and a passive thermal-regulation system based on a network of single-shelf unregulated ammonia heat pipes under the conditions of orbital operation, carried out within the framework of the dynamic traditional LPTMM and more complex DLPTMM, has shown their fairly good agreement as far as the most important calculated parameters are concerned for a minimum number of subdivisions of (5×5). In this connection, the traditional dynamic LPTMM with such a number of subdivisions and a low consumption of time makes it possible to predict with a sufficient degree of accuracy the external and internal radiative heat exchange, the thermal regimes of the onboard devices from the maximum and minimum temperatures at the mounting sites, and the parameters of the passive thermal-regulation system based on a network of single-shelf unregulated ammonia heat pipes of an NS. A more complex and perfect dynamic DLPTMM of the payload module of an NS is recommended for monitoring of thermal analyses within the framework of dynamic LPTMMs, a detailed evaluation of the degree of nonuniformity of the temperature fields at the mounting sites of onboard equipment with an inhomogeneous heat release and a narrow permissible range of normal-operation temperatures, and prediction of the thermoelastic stressed-strained state of the honeycomb structure of the instrument compartment.

NOTATION

a, thermal-diffusivity coefficient, m^2/sec; A_s, integral (total) hemispherical absorptivity; $Bi_{f.h} = \alpha_{f.h}\delta_h/\lambda_{eff}$, Biot number of contact heat exchange through the adhesive joint between the facing and the honeycomb filler; *c* and *C*, specific heat and total heat capacity, J/(kg·K) and J/K; E_r, density of the resulting radiative heat flux, W/m^2; Γ, boundary; *F*, area, m^2; *h*, height, m; L_x and L_y, linear dimensions of the panel, m; *n*, external normal; $N_{h.p}$ and $N_{s.e}$, number of heat pipes and onboard devices; N_x and N_y, number of nodes into which a three-layer panel is subdivided along the axes of the Cartesian coordinate system; *P*, heat-release power of the device, W; *q*, heat-flux density, W/m^2; $\underline{Q_m}$, source term in (11), K/sec; S_0, density of the flux of direct solar radiation, W/m^2; *t*, time, sec; *T*, temperature, K; $\overline{T}$, mean-integral temperature, K; Φ_m and $\Phi_{m\,cont}$, source terms in (12), K/sec; *x*, *y*, Cartesian coordinates, m; α, coefficient of contact thermal conductivity, $W/(m^2·K)$; δ, thickness, m; ε, integral (total) hemispherical emissive power; θ, angle between the normal to the North and South instrument-radiator panels and the direction to the sun; λ, thermal-conductivity coefficient, W/(m·K); ρ, density, kg/m^3; ξ, marching coordinate along the perimeter (skeleton elements) of the honeycomb panel, m; σ, thermal conductance, W/K; σ_0, Stefan–Boltzmann constant, $W/(m^2·K^4)$. Subscripts: cont, contact of two honeycomb panels via the skeleton elements; cond, conductive; c, condensation zone; r, radiative; eff, effective; e, evaporation zone; f, facing; f.h, contact of the facing with the honeycomb filler; f.st, contact of the facing with the skeleton element; f.p, contact of the facing with the heat pipe; h, honeycomb filler; h.p, heat pipe; *i*, ordinal number of computational nodes; int, initial conditions; *m*, ordinal number of a neighboring computational node; *n*, ordinal number of the node of a heat pipe in the evaporation (condensation) zone; p.p, contact of two heat pipes; s.e, onboard device (spacecraft equipment); st, skeleton elements; s, direct solar radiation; v, saturated vapor; 1 and 2, load-bearing facings; 3, 4, 5, and 6, elements of the skeleton of a three-layer honeycomb panel; 1, 2, and 3, heat pipes in the South, Central, and North panels in (5)–(10); max, maximum; min, minimum.

REFERENCES

1. E. A. Ashurkov, V. P. Kozhukhov, A. G. Kozlov, E. N. Korchagin, V. V. Popov, and M. F. Reshetnev, *Spacecraft of a Block-Modular Type*, Patent No. 2092398 MKI B 6461/10, Byull. No. 28, published on 10.10.97.
2. V. A. Burakov, E. N. Korchagin, V. P. Kozhukhov, et al., Mathematical simulation of heat exchange in a nonhermetic instrumental compartment of a spacecraft, *Inzh.-Fiz. Zh.*, **73**, No. 1, 113–124 (2000).
3. B. M. Pankratov, *Thermal Design of Flying-Vehicle Units* [in Russian], Moscow (1981).
4. V. M. Zaletaev, Yu. V. Kapinos, and O. V. Surguchev, *Calculation of the Heat Transfer of a Spacecraft* [in Russian], Moscow (1979).
5. V. M. Popov, *Heat Transfer through Adhesive Joints* [in Russian], Moscow (1974).
6. Yu. P. Shlykov and E. A. Ganin, *Contact Thermal Resistance* [in Russian], Moscow (1977).
7. N. N. Yanenko, *Subincremental Method for Solving Multidimensional Problems of Mathematical Physics* [in Russian], Novosibirsk (1967).
8. A. A. Samarskii, *The Theory of Difference Schemes* [in Russian], Moscow (1983).